High-yield production of mono- or few-layer transition metal dichalcogenide nanosheets by an electrochemical lithium ion intercalation-based exfoliation method

Ruijie Yang, Liang Mei, Qingyong Zhang, Yingying Fan, Hyeon Suk Shin, Damien Voiry, Zhiyuan Zeng

▶ **To cite this version:**

HAL Id: hal-03873245

https://hal.umontpellier.fr/hal-03873245

Submitted on 26 Nov 2022

High-yield production of mono- or few-layer transition metal dichalcogenides nanosheets by electrochemical lithium ion-intercalation and exfoliation method

Ruijie Yang[a†], Liang Mei[a†], Qingyong Zhang[a†], Yingying Fan[a], Hyeon Suk Shin[b*], Damien Voiry[c*], Zhiyuan Zeng[a*]

[a]Department of Materials Science and Engineering, City University of Hong Kong, 83 Tat Chee Avenue, Kowloon, Hong Kong 999077, P. R. China.
[b]Department of Chemistry, Ulsan National Institute of Science and Technology (UNIST), Ulsan 612022, South Korea.
[c]Institut Européen des Membranes, IEM, UMR 5635, Université Montpellier, ENSCM, CNRS, Montpellier.

Authors:

R.J. Yang (E-mail: ruijyang@cityu.edu.hk).

L. Mei (E-mail: liangmei2-c@my.cityu.edu.hk).

Q.Y. Zhang (E-mail: qzhang449-c@my.cityu.edu.hk).

Y.Y. Fan (E-mail: 1005755945@qq.com).

Corresponding authors:

Dr. Z.Y. Zeng (E-mail: zhiyzeng@cityu.edu.hk; Tel. Number: +852-34422318; Fax Number: +852-34420892; Lab Website: https://www.zeng-lab.com).

Dr. D. Voiry (E-mail: damien.voiry@umontpellier.fr; Tel. Number: +33-467-61-9115; Lab Website: https://lowdimensional-materials.net).

Prof. H.S. Shin (E-mail: shin@unist.ac.kr; Tel. Number: +82-52-217-2311; Lab Website: http://lnn.unist.ac.kr).

† Ruijie Yang, Liang Mei, and Qingyong Zhang contributed equally to this work.

Abstract

Transition metal dichalcogenides (TMDs) nanomaterials, especially the mono- or few-layer ones, have received extensive research interest owing to their suitable band-gap, unique electronic structure, outstanding biocompatibility, excellent stability, and promising catalytic properties. Therefore, the reliable production of these nanomaterials with atomically thin thickness and laterally uniform dimension are essential for their promising applications in transistors, photodetectors, electroluminescent devices, catalysis, energy conversion, environment remediation, biosensing, bioimaging, and so on. Recently, the electrochemical lithium ion-intercalation and exfoliation method has emerged as a mature, efficient and promising strategy for the high-yield production of mono- or few-layer TMDs nanosheets; mono-layer MoS_2 (yield of 92%), mono-layer TaS_2 (yield of 93%) and bi-layer TiS_2 (yield of 93%) with lateral dimensions of around 1 μm. This Protocol describes the details of experimental procedures for the high-yield synthesis of mono- or few-layer TMDs and other inorganic nanosheets such as MoS_2, WS_2, TiS_2, TaS_2, ZrS_2, graphene, h-BN, $NbSe_2$, WSe_2, Sb_2Se_3, and Bi_2Te_3 by using the electrochemical lithium ion-intercalation and exfoliation method which involves the electrochemical intercalation of lithium ions into the layered inorganic crystals and a mild sonication. In addition, this method offers some more advantages such as the control over the nature of the crystal polytypes. The whole protocol takes 26-38 h for the successful production of the final ultrathin inorganic nanosheets.

Introduction

Transition metal dichalcogenides (TMDs) nanomaterials, especially the mono- or few-layered crystals, have received extensive research interest owing to their unique properties associated with various kinds of promising applications in transistors, photodetectors, electroluminescent devices, catalysis, energy conversion, environment remediation, biosensing, bioimaging, and so on[1-20]. Their unique properties provide opportunities to go beyond those of graphene[21]. Therefore, the reliable production of these nanomaterials with atomically thin and uniform properties is of high importance both fundamentally and practically. Recent advances in synthesis technologies of

ultrathin 2D nanomaterials have enabled the fabrication of mono- or few-layered TMDs nanomaterials via various synthesis approaches, including mechanical cleavage[22-25], chemical vapour deposition (CVD) growth[26-34], molecular beam epitaxy (MBE)[35-38], wet-chemical synthesis[39,40], liquid intercalation[13,41-52], and so on. However, preparing high-quality and high-yield mono- or few-layered TMDs nanosheets under mild conditions remains a challenge. For example, ultrathin 2D TMDs nanosheets fabricated using mechanical cleavage are plagued by the low-yield of the products and the difficulty for the controlling of the thickness, size, and shape of the 2D TMDs nanosheets. In terms of CVD growth, its working environment is relatively harsh, always needs high temperature and high vacuum, which are not always compatible with the targeted applications. Regarding wet-chemical synthesis, the limitation is that the synthesis process is easily affected by the reaction conditions (*e.g.*, temperature, time, types and concentrations of precursors, solvents, and surfactant), which leads to the uncontrollability for fabrication of the 2D TMDs nanosheets. Besides, TMDs fabricated by liquid exfoliation show an intrinsically broad thickness distribution, leading to poor film quality and unsatisfactory thin-film electrical performance.

Motivated by these, our group has developed an electrochemical lithium ion-intercalation and exfoliation strategy for the fabrication of mono-layer TMDs nanomaterials with better quality and high-yield (> 90%) under mild conditions (at room temperature), also with relative short time[53-56]. In 2011, our group first reported the electrochemical lithium ion-intercalation and exfoliation synthesis of mono-layer MoS_2, WS_2, TiS_2, TaS_2, ZrS_2 and graphene nanosheets, and achieved the 92% yield for mono-layer MoS_2[53]. Meanwhile, by regulating the cut-off voltage and discharge current in the synthesis process, few-layer-thick BN, $NbSe_2$, WSe_2, Sb_2Se_3, and Bi_2Te_3 were also obtained[54]. In addition, the high-yield production of mono-layer TaS_2 (93%) and bi-layer TiS_2 (93%) was achieved *via* the optimization of the electrochemical intercalation condition[55]. Note that the statistics atomic force microscope (AFM) measurements were conducted by testing large quantity (> 100 pieces for each TMD) of TMDs nanosheets, and the results shows that 92% of MoS_2 and 93% of TaS_2

nanosheets are mono-layers (< 1 nm), and 93% of TiS_2 nanosheets are bi-layers (< 2 nm). To the best of our knowledge, until now, besides our work, no other route of exfoliation allows obtaining such high yield production of mono-layer MoS_2, TaS_2 and bi-layer TiS_2 through a general exfoliation method. Here, the key parameter to determine whether producing mon-, bi- or few- layer TMDs nanosheets is the lithium intercalation extent in layers, if every layer is intercalated with lithium ions, then mon-layer will be produced after exfoliation, if only parts of the layers are intercalated with lithium ions, then bi- or few-layer will be synthesized. Furthermore, TiS_2-based hetero-nanostructures, such as TiS_2-CuS, TiS_2-ZnS and TiS_2-Ni_3S_2 have also been obtained via this method, by using the layered TiS_2 coated copper (for preparation of TiS_2-CuS), zinc (for preparation of TiS_2-ZnS) and nickel (for preparation of TiS_2-Ni_3S_2) foil discs as cathodes, respectively[56].

Importantly, compared with the traditional chemical ion-intercalation and exfoliation method for the fabrication of mono- or few-layer TMDs nanosheets, our developed electrochemical ion-intercalation and exfoliation method is relatively simple, straightforward and offer a higher degree of control under a mild condition. The traditional chemical ion-intercalation and exfoliation method, which uses n-butyl lithium in hexane as the intercalation agent, needs to be carried out at relatively high temperature (*e.g.,* 100 °C) for long time (*e.g.,* 3 days) and lacks the controllability over the amount of Li insertion. Incomplete lithium intercalation will result in low yield of mono-layer production, while excessive lithium insertion will lead to the chemical decomposition of the crystals. Our developed electrochemical ion-intercalation and exfoliation method for the high-yield preparation of mono-layer TMDs nanosheets can be easily conducted at room temperature within 26 h. In addition, the Li insertion can be monitored and finely controlled using the battery testing equipment and exhibited in the form of galvanostatic discharge curves, and the galvanostatic discharge can be stopped at a proper Li content to avoid decomposition of the intercalated compounds. Besides the improved feasibility and effectiveness in the methodology, our procedure is also scalable, and we believe that further scale-up production of mono-layer TMDs

nanosheets for industry applications can be realized by increasing the bulk TMDs amount from milligrams (mg) to gram (g), or even to ton. Also, the lateral size of the exfoliated mon-layer nanosheets can be further increased from around 1 μm, to higher than 1 μm by increasing the lateral size of TMDs bulk materials. Interestingly, the phase transition of TMDs from the semiconducting 2H phase to the metallic 1T phase during the exfoliation process was achieved, which offers great opportunities towards phase engineering of TMDs, in order to realize superior performance for some emerging applications in electronics or electro-catalysis.

In this Protocol, we systematically describe the detailed experimental procedures of our established electrochemical lithium ion-intercalation and exfoliation strategy for the synthesis of mono- or few-layer inorganic nanosheets, including MoS_2, WS_2, TiS_2, TaS_2, graphene, h-BN, $NbSe_2$, WSe_2, Sb_2Se_3, and Bi_2Te_3. Our aim is to increase the general understanding of this exfoliation route for the efficient synthesis of ultrathin TMDs nanosheets and thus benefit the community from their various potential applications. In addition, it will also promote the fabrication of some other ultrathin 2D nanomaterials with atomic level thickness besides TMDs, such as black phosphorus, g-C_3N_4, metal oxides[57-59] etc. We also believe that this protocol will attract a broad research interest from chemists, material scientists, crystallographers, photoelectric device manufacturer, catalysis researcher, bioscientist *etc.*

Applications:

Our developed electrochemical lithium ion-intercalation and exfoliation method for the high-yield production of mono- or few-layer TMDs nanosheets has opened a new direction for basic and applied research, attracting the attention of both academia and industry[60]. The prepared mono- or few-layer TMDs nanosheets by this method has been wildly applied in various fields such as gas-sensing[61], memory devices[62], detection of biomolecules[63], electrocatalytic hydrogen evolution[55,64,65], light-emitting diodes[66], and lithium-ion battery[56,67]. Based on a literature survey using Web of Science, the past few years have witnessed a

continuation in the upward trend to adopt our developed method for the fabrication of mono- or few-layer TMDs nanosheets, due to the specificity, timeliness and innovation of this method.

Limitations:

To date, mono layer (< 1 nm) MoS_2, WS_2, TiS_2, TaS_2, ZrS_2, and graphene nanosheets as well as several multi-layer (< 4 nm) BN, $NbSe_2$, WSe_2, Sb_2Se_3, and Bi_2Te_3 nanosheets have been successfully fabricated by our electrochemical lithium ion-intercalation and exfoliation method. While, as for the synthesis of other mono- or few-layered 2D nanomaterials, such as $MoSe_2$, VSe_2, black phosphorus, g-C_3N_4, substantial modifications of the protocol might be necessary. Furthermore, in spite of the interesting phase transformation of TMDs from the semiconducting 2H phase to the metallic 1T or distorted 1T' phase during the exfoliation process, the switch of phase transition has not been fully controlled. Previous crystal field theory explained that the intercalation of ions involves the transfer of electron from the *s* orbitals of guest ions to the *d* orbitals of the host transition-metal atoms[68-70]. The injection of electron beyond a certain threshold causes the stability of 2H phase to be lower than that of 1T or 1T′ phase, inducing the corresponding phase transitions. Although the mechanism of phase transformation is clear, the control is still challenging. We will continue devoting our efforts toward the precise and purposeful control of phase modulation during the preparation of mono- or few-layer TMDs nanosheets by our developed electrochemical lithium ion-intercalation and exfoliation method, to realize the controllable synthesis of high purity phase.

Experimental design:

The mono- or few- layer inorganic nanosheets in this protocol, are synthesized by the electrochemical lithium ion-intercalation and exfoliation method, which involves the electrochemical intercalation of lithium ion into layered bulk materials,

followed by a mild sonication and exfoliation process in solvent (**Fig. 1**).

The electrochemical lithium ion-intercalation process of the layered bulk materials is carried out in a test coin cell using Li foil as anode, copper (Cu) foil with uniformly coated layered bulk material as cathode, polypropylene (pp) film as the separator, and 1.0 M $LiPF_6$ in a mixture of ethyl carbonate (EC) and dimethyl carbonate (DMC) (with 1:1 volume ratio)) solution as electrolyte. The prepared coin cell is discharged by connecting it to a Neware battery test system with a galvanostatic discharge current of 0.05 mA or 0.025 mA and a controlled cut off voltage at room temperature. During such a discharge process, lithium ions are inserted into the interlayer of the layered bulk materials, resulting in the enlarging of interlayer spacing and the weakening of interlayer van der Waals interaction. Such changes of interlaminar properties will make the subsequent exfoliation process easier to realize. Importantly, the amount of lithium intercalation can be effectively controlled by tuning the cut-off voltage (or the discharge capacity). This superior feature can make the lithium intercalation process stop at an appropriate lithium amount, avoiding the decomposition of lithium intercalated compounds.

After lithium intercalation, dismantle the coin cell and take out the Cu foil, whose surface coated with lithium intercalation compound materials, then wash it with acetone to remove the residual electrolyte (i.e., $LiPF_6$), and dry it. The lithium-intercalated compound materials on the surface of Cu foil are then immersed in deionized (DI) water (or ethanol) and sonicated for 5 -10 min. After that, the opaque suspension of the exfoliated materials will be obtained.

During the lithium ion battery discharging process, the lithium ions, released from lithium metal anode, inserted into the interlayer spaces of layered bulk cathode materials, play dual roles. First, after intercalation, the lithium ions get electrons from lithium metal anode through external circuit (battery testing equipment) and reduced to lithium atom between the Van der Waals gaps of the layered materials. Second, the intercalated lithium metal atoms in between layered materials react

7

with DI water (H_2O) to form lithium hydroxide (LiOH), along with the releasing of hydrogen (H_2) gas (evidently bubbles can be observed during the ultrasound process in water), which will expand the interlayer distance and weaken the van der Waals interactions between the layers and thus help the layers separate. Note that, there are remaining charges (lithium ions) on the nanosheets after the exfoliation process, which has been confirmed using Zeta potential measurements and estimated to be 15 to 20 % in the case of group-6 TMDs[71]. Such remaining charges of the exfoliated materials induces a stabilization of the suspension by increasing the entropy of the system[72].

After exfoliation of the intercalated layered materials in H_2O, the obtained opaque suspensions are centrifuged and washed 1 ~2 times to get the final 2D nanosheets for transmission electron microscope (TEM), atomic force microscope (AFM), X-ray photoelectron spectroscopy (XPS), Raman, and ultraviolet–visible spectroscopy (UV-Vis) characterizations. TEM is used to investigate the crystal structure, morphology and size of the exfoliated materials. AFM can directly measure the thickness and size of the 2D nanosheets and help to determine the mono-layer yield. XPS is used to determine the elemental composition and valence of the exfoliated nanosheets. Raman is used to deduce electronic structure. UV-Vis can provide information about the photon absorption property. In this protocol, we describe how to prepare this mono- or few- layer nanosheets for these characterizations as well as how to use these analytical methods to analyze the properties of the exfoliated counterparts.

Materials

Reagents:

! CRITICAL: Store the bulk inorganic layered materials (e.g., MoS_2, WS_2, TiS_2, TaS_2, Natural graphite, BN, $NbSe_2$, WSe_2, Sb_2Se_3, and Bi_2Te_3) in Ar-filled glove box, because they are easily deliquesced in air. Meanwhile, keep them away from light by wrapping the bottle of bulk inorganic layered materials in aluminum foil.

• Molybdenum disulfide (MoS_2; 10-30 μm, Rose Mill, West Hartford, USA, cat. no. C10404842).

• Tungsten (IV) disulfide (WS_2, Sigma, Steinheim, Germany, cat. no. C10534199)

• Titanium (IV) sulfide (TiS_2, Sigma, Steinheim, Germany, cat. no. MKCH8948)

• Tantalum (IV) sulfide (TaS_2, Alfa Aesar, Massachusetts, USA, cat. no. 808717)

• Zirconium (IV) sulfide (ZrS_2, Strem, Massachusetts, USA, cat. no. 808679)

• Natural graphite (Bay carbon Inc, Michigan, USA, cat. no. 43319)

• Boron nitride (BN, Sigma, Steinheim, Germany, cat. no. 112073)

• Niobium selenide ($NbSe_2$, Alfa Aesar, Massachusetts, USA, cat. no. S08E024)

• Tungsten (IV) selenide (WSe_2, Alfa Aesar, Massachusetts, USA, cat. no. 808822)

• Antimony triselenide (Sb_2Se_3, Sigma, Steinheim, Germany, cat. no. 401196)

• Bismuth telluride (Bi_2Te_3, Sigma, Steinheim, Germany, cat. no. 733482)

• Poly(vinylidene fluoride) (PVDF, Sigma, Steinheim, Germany, cat. no. FCB036778)

• Polypropylene (pp) film (Celgard 2300, North Carolina, USA)

• N-methylpyrrolidone (NMP, Sigma, Steinheim, Germany, cat. no. LI40T113)

• 3-aminopropyltriethoxysilane (APTES, Sigma, Steinheim, Germany, cat. no. C2002164)

• Sulphuric acid (H_2SO_4, Sigma-Aldrich, Germany, cat. no. 109072)
! CAUTION: Personal protective equipment must be worn during experiments involving H_2SO_4, as it is strong acids and can cause skin burns.

• Hydrogen peroxide solution (H_2O_2, Sigma-Aldrich, Germany, cat. no. 107209)

• Lithium-ion battery electrolyte (Suzhou Duo Duo Chemical Technology Co., Ltd, China, cat. no. LB064)

• Lithium foil (Fisher Scientific Company, Canada, cat. no. AA1076914)

• The copper foil (Aritech Chemazone Private Limited, India, cat. no. NCZ-MN-177/20)

• Acetone (Anaqua Global International Inc. Limited, USA, cat. no. TAE11Y1708TH)

• Ethanol (>99.9 %, Merck, Darmstadt, Germany, cat. no. C10654595)

• Deionized water (H_2O; Milli-Q System; Millipore)

Equipments:

• Digital hotplate stirrers (Stuart Equipment, cat. no. UC152D)

• Vacuum drying oven (Shanghai Yiheng Scientific Instrument Company, cat. no. 190728051)

• Precision disc cutting machine (Shenzhen Kejngstar Technology Company, cat. no. PE01219G2163)

• Infrared heating tape casting coater (Shenzhen Kejngstar Technology Company, model no. MSK-AFA-ES200)

• Compact hydraulic crimping machine (Shenzhen Kejngstar Technology Company, cat. no. PE00320L3807)

• Coin cell shell (Taizhou Yajun Battery Material Co., Ltd, China, cat. no. CR2032)

• Glove box (Vigor Gas Purification Technologies (Suzhou) Co., Ltd, model no.

SG2400/750TS)

• NEWARE battery test system (CT-ZWJ-4'S-T-1U, cat. no. T1906-200654)

• Glass vials (5 and 25 ml) with appropriate polyethylene snap caps (VWR Collection, cat. nos. 548-0141 and 548-0144)

• Parafilm (Parafilm, cat. no. PM996)

• Disposable plastic dropper (Kangjian, cat. no. KJ 619)

• Scissors

• Three micropipettes (ranges: 0.5-10, 10-100 and 100-1,000 μl) with appropriate disposable tips

• Polypropylene microcentrifuge tubes (1.5 and 2.0 ml; Axygen, cat. nos. MCT-150-C and MCT-200-C)

• Microcentrifuge (Thermo Scientific, cat. no. 75002466)

• Ultrasonic cleaning bath (Branson Ultrasonic, cat. no. CPX-952-238R)

• Transmission electron microscope (TEM; JEOL, model no. JEOL-2100F)

• Holey carbon-coated copper grids (200 mesh) for TEM sample preparation

• Atomic force microscope (AFM; Veeco, model no. Dimension 3100)

• APTES-modified Si/SiO_2 substrate for AFM characterization

• X-ray photoelectron spectrometer (Ulvac-Phi, model no. PHI5000 Versaprobe III)

• Raman spectrometer (HORIBA Jobin Yvon S.A.S., model no. LabRAM HR Evolution)

• Ultraviolet-visible spectrophotometer (Shimadzu, model no. Ultraviolet 2450)

Equipment Setups:

Electrochemical lithium ion-intercalation setup

• This setup consists of a coin cell, and a Neware battery test system. Such a coin cell uses Li foil as anode, copper (Cu) foil with uniformly coated layered bulk material as cathode, polypropylene (pp) film as the separator, and 1.0 M $LiPF_6$ in a mixture of ethyl carbonate (EC) and dimethyl carbonate (DMC) (with 1:1 volume ratio)) solution as electrolyte. Note that the coin cell should be assembled in a glove box filled with Ar. The prepared coin cell is connected with the Neware battery test system and discharged with a galvanostatic discharge current of 0.05 or 0.025 mA and a cut-off voltage of 0.9 V (ZrS_2: 0.7 V, BN: 0.4 V, Graphite 0.1V) at room temperature. A typical setup is shown in **Fig. 2**. Note that, the amount of intercalated lithium ions in layered materials (or the discharge capacity) can be effectively controlled by tuning the cut-off voltage according to the discharge profile. Because the discharge capacity can transform into lithium intercalation amount by calculating and substituting the discharge capacity that corresponding to 1 Moore lithium intercalation for different kinds of inorganic layered materials, as shown in **Supplementary Table 1.**

TEM setup

• In this protocol, TEM characterization is carried out on a JEOL JEM-2100F TEM instrument under the accelerating voltage of 200 kV. The TEM samples are prepared by dropping the as-prepared mono- or few- layer inorganic nanosheets solution onto lacey carbon 300 mesh copper TEM grids and then dried in air.

AFM setup

• In this protocol, AFM characterization is carried out on a Veeco Dimension

3100 AFM instrument under the tapping mode and with a Si tip (spring constant: 42 N/m; resonance frequency: 320 kHz). The AFM samples are prepared by dropping the as-prepared mono- or few- layer inorganic nanosheets solution onto an APTES-modified Si/SiO$_2$ substrate and then dried in air.

Procedure

Synthesis of mono- or few- layer TMDs nanosheets (Timing 26 h):

1. Prepare the mixed slurry of layered bulk material, acetylene black, PVDF and NMP. Weigh out 200 mg of layered bulk material (i.e., MoS$_2$, WS$_2$, TiS$_2$, TaS$_2$, ZrS$_2$, graphite, BN, NbSe$_2$, WSe$_2$, Sb$_2$Se$_3$, or Bi$_2$Te$_3$), 25 mg of acetylene black, and 25 mg PVDF into a 10-mL glass vial, and then add 1.6 mL NMP and a rotor. After heating the vial in 60 °C oven for 30 min, put the mixed slurry contained 10-mL glass vial on magnetic stir plate and stir the mixed slurry for 7.5 h. (Timing 8 h)

! CRITICAL STEP: The mixed slurry needs to be stirred in a closed vial with good sealability because the slurry is easy to adsorb water.

2. Uniformly coat the obtained mixed slurry on one side of a copper foil using an infrared heating tape casting coater. Then put it into a vacuum drying oven and dry it at 100 °C under vacuum for 8 h. After drying, using precision disc cutting machine cut it into disc with diameter of 1.2 cm for next coin cell assembling. (Timing 8 h)

3. Assemble the coin cell in an Ar-filled glove box (**Fig. 3a**). (Timing 1 h)

   (I) Put the stainless steel cap on a piece of white paper.

   (II) Put the TMDs bulk materials coated copper discs (with diameter of 1.2 cm), in the cap.

(III) Put the polypropylene (pp) film (with diameter of 1.6 cm) on the top of Cu discs.

(IV) Use 20 µL pipette gun to apply 4µL electrolyte on the polypropylene (pp) film.

(V) Put the lithium foil (with diameter of 1.4 cm), gasket, stainless steel shrapnel and aluminum coated cup on the top in turn.

(VIII) Press it using punching machine with 500 psi, and then the cell is ready for testing.

Take out the pressed coin cell and let the electrolyte soak the electrode thoroughly for 4 hours.

! CRITICAL STEP: The water content in glove box should be extremely low, because the lithium foil is very sensitive to water.

4. Started the galvanostatic discharge process (**Fig. 3b**). Connect the obtained coin cell to the battery test system. Then, set up current density at 0.05 mA or 0.025 mA, and cut-off voltage at 0.9 V (ZrS$_2$: 0.7 V, BN: 0.4 V, Graphite 0.1V). Press the start button to start the discharge process. After reaching the cut-off voltage, remove the coin cell from the battery test system and let the lithium intercalated electrode relax for 1 h. (Timing 7 h)

! CRITICAL STEP: The discharge current and cutoff voltage are very important for electrochemical Li intercalation process. High discharge current may induce the structure degradation but can shorten reaction time. Low discharge current will require much time to finish the intercalation but can avoid structure degradation. High cutoff voltage may cause the insufficient lithium intercalation and thus not good exfoliation efficiency. While low cutoff voltage will result in the structure degradation. In this protocol, for MoS$_2$, discharge current is 0.05 mA, cutoff voltage is 0.9 V. For TaS$_2$, TiS$_2$, WS$_2$, discharge current is 0.025 mA, cutoff voltage

is 0.9 V. For ZrS$_2$, discharge current is 0.025 mA, cutoff voltage is 0.7 V. For graphene, discharge current is 0.025 mA, cutoff voltage is 0.1 V. For BN, discharge current is 0.025 mA, cutoff voltage is 0.4 V. For NbSe$_2$, discharge current is 0.025 mA, cutoff voltage is 0.7 V. The corresponding galvanostatic discharge curves are shown in **Supplementary Fig. 1**. *About how to determine these cut-off voltages for different materials, our explanation is as follows: for the materials that show obvious discharge plateau in galvanostatic discharge curve (such as MoS$_2$. etc), the cut-off voltage should be a little lower than the platform voltage. While, for those without discharge plateau in discharge curve, SEM, TEM and AFM should be systematic combined for characterization of the product obtained under different cut-off voltage, to see its morphology (nanosheets or decomposed nanoparticles) and thickness, thus to determine whether the selected cut-off voltage is suitable for this product.*

5. Disassemble the coin cell and take out the TMDs coated copper foil after Li-intercalation (**Fig. 3c**). Then wash it immediately with acetone to remove any residual electrolyte (LiPF$_6$/EC/DMC). Then immerse the TMDs coated copper foil in a 10-mL glass vial containing 10 mL distilled water or ethanol (**Fig. 3d**). Then, put the 10-mL glass vial into the ultrasonic pool and ultrasonic for 5 min with 28 KHz. After that, an opaque suspension of the exfoliated mono or few layer nanosheets is formed. (Timing 10 min)

! CRITICAL STEP: After taking out the copper foil loaded with Li-intercalated sample from the coin cell, this washed process should be quick, and immediately perform the next exfoliation step, because the Li-intercalated sample is sensitive to the environment. For NbSe$_2$, WSe$_2$, Sb$_2$Se$_3$, and Bi$_2$Te$_3$, it is better do N$_2$ bubbles treatment for DI water in the glass vial before the ultrasonication process, this process can remove the dissolved oxygen in DI water and alleviate the surface oxidation for the exfoliated TMDs nanosheets in the dispersion.

! TROUBLESHOOTING

6. Started the centrifugal washing process (**Fig. 3e**). Put the obtained opaque suspension into 20-mL centrifuge tube. Centrifuge it for 15 min with 2000 rpm. Then collect the supernatant into a new 20-mL centrifuge tube. Centrifuge it for 15 min with 10000 rpm. Then pour the supernatant away, leaving the bottom sedimentation, followed by re-disperse and the sedimentation in newly added DI water and doing 10000 rpm centrifuges for 1 ~ 2 times. Then collect the bottom sedimentation of the last centrifugation (the final products) into a 10-mL glass vial. Finally, redisperse the collected sediment into opaque suspension by adding water or ethanol, and store this opaque suspension for use.

! CRITICAL STEP: The centrifugal speed affects the quality of final products. Too low centrifugation speed in first step is not enough to remove the un-exfoliated TMDs materials, acetylene black and PVDF. A too high centrifugation speed in first step causes the mono or few layer nanosheets loss as well. A too low centrifugation speed in second step induces the mono or few layer nanosheets loss, since they all not completely centrifuged to bottom and exited as sedimentation. While a too high centrifugation speed in second step results in obtained nanosheets too small in lateral size.

! PAUSE POINT: The obtained mono or few layer TMDs nanosheets can be stored at room temperature under dry and dark condition for several months without noticeable change.

TEM characterization of the obtained mono- or few- layer TMDs nanosheets (Timing 3 h):

7. Take 0.5 mL mono or few layer TMDs nanosheets collected from step 6 into 2-mL glass vial and add 1.5 mL water to dilute the TMDs nanosheets dispersion. Then, shake the glass vial to obtain a homogeneous TMDs nanosheets solution.

8. Deposit 5 μL of this solution onto a lacey carbon-coated copper grids and let it dry in air for 15 min before the characterization.

9. Image the exfoliated mono or few layer TMDs nanosheets by using a JEOL JEM-2100F TEM instrument.

AFM characterization of the obtained mono- or few- layer TMDs nanosheets (Timing 5 h):

10. Prepare APTES-modified Si/SiO$_2$ substrate.

(I) Put Si/SiO$_2$ substrate (10 mm × 8 mm) into acetone and sonicate for 5 min. Take the substrate out from acetone and rinse it with DI water.

(II) Then put the Si/SiO$_2$ substrate into piranha solution (volume ratio H$_2$SO$_4$: H$_2$O$_2$ = 7:3) and heat the mix solution to boiling point for 30 min (hot plate temperate 120 °C).

(III) Take out the Si/SiO$_2$ substrate, rinse it with DI water using wash bottle and blow it using N$_2$ gas to dry the substrate.

(IV) Immerse the obtained Si/SiO$_2$ substrate in APTES solution (volume ration APTES: H$_2$O = 1:100), and put it into the vacuum condition for 10 min. Then take out the Si/SiO$_2$ substrate, rinse it with DI water and blow it using the N$_2$ gas.

(V) Then put this Si/SiO$_2$ substrate in 120 °C oven for 2 h to get the final APTES-modified Si/SiO$_2$ substrate.

! CRITICAL STEP: APTES functionalization is critical for the successful AFM measurement. APTES is positively charged on the surface, which is beneficial for electrostatic adsorption of the negatively charged TMDs nanosheets. Otherwise, the TMDs nanosheets are easily aggregated through drop casting on Si/SiO$_2$ substrate. Without APTES functionalization, the AFM measurement of TMDs nanosheets is not easily succeed, especially for the single-layer or few layers nanosheets.

11. Take 0.5 mL mono or few layer TMDs nanosheets collected in step 6 into 2-mL

glass vial and add 1.5 mL DI water. Then, shake the glass vial to obtain a homogeneous TMDs nanosheets solution.

12. Put the APTES-modified Si/SiO$_2$ substrate (Prepared in step 10) into the 2-mL glass vial containing homogeneous TMDs nanosheets solution (prepared in step 11) and immerse it in solution for 15 min. Then, take Si/SiO$_2$ substrate out and rinse it with DI water. After that, blow substrate use the N$_2$ gas for 5 min.

13. Image the obtained mono or few layer TMDs nanosheets by using a Veeco Dimension 3100 AFM instrument.

! TROUBLESHOOTING

XPS and Raman characterizations of the obtained mono- or few- layer TMDs nanosheets (Timing 3 h):

14. Take 0.5 mL opaque suspension of mono or few layer TMDs nanosheets collected from step 6 onto Si/SiO$_2$ substrate (5 mm * 5 mm) and let it dry in air for 2 h before the XPS and Raman characterizations.

15. Test the XPS curves of the exfoliated mono or few layer TMDs nanosheets using a PHI5000 Versaprobe III X-ray photoelectron spectrometer.

16. Test the Raman curves of the exfoliated mono or few layer TMDs nanosheets using a LabRAM HR Evolution Raman spectrometer.

UV-Vis characterization of the obtained mono- or few- layer TMDs nanosheets (Timing 0.5 h):

17. Take 3.0 mL opaque suspension of mono or few layer TMDs nanosheets collected from step 6 into 3.5 mL quartz cuvette.

18. Test the UV-Vis curves of the exfoliated mono or few layer TMDs nanosheets using an Ultraviolet-2450 ultraviolet-visible spectrophotometer.

Troubleshooting

Troubleshooting advice can be found in **Table 1**.

Table 1 Troubleshooting table

Step	Problem	Possible causes	Solution
5	Sometimes, the layered bulk materials are not fully exfoliated, some of the bulk particles can be clearly seen in solution.	The discharging time is not enough or there are some short circuit in the battery.	Make sure that the separator is completely separating the cathode and anode in step 3.
13	Lots of particles are observed in AFM images.	Too long ultra-sonication time will cause 2D nanosheets break into small particles and then aggregate to large particles in in step 5. The TMDs nanosheets are not washed enough in step 6.	Reduce the ultra-sonication time. Also use the DI water to wash the nanosheets 1 ~ 2 times.

Timing

Steps 1-6, Synthesis of mono- or few- layer inorganic nanosheets: 26 h

Steps 7-9, TEM characterization of the obtained mono- or few- layer inorganic nanosheets: 3 h

Steps 10-13, AFM characterization of the obtained mono- or few- layer inorganic nanosheets: 5 h

Steps 14-16, XPS and Raman characterizations of the obtained mono- or few- layer inorganic nanosheets: 3.5 h

Steps 17-18, UV-Vis characterization of the obtained mono- or few- layer inorganic nanosheets: 0.5 h

Anticipated results

After sonication treatment (Step 5), an opaque suspension of the exfoliated materials should be obtained (**Fig. 4**). After the whole electrochemical lithium ion-intercalation and exfoliation processes, the mono layer (thickness < 1 nm) MoS_2, WS_2, TiS_2, TaS_2, and multi-layers (thickness < 4 nm) BN, $NbSe_2$ nanosheets can be obtained (**Fig. 5 and Fig. 6**) with high yield (MoS_2 and TaS_2 mono layer & TiS_2 double layer yield > 90%) (**Fig. 7**) (**Supplementary Table 2**). Besides, mono layer (thickness < 1 nm) ZrS_2 and graphene nanosheets, as well as multi-layers (thickness < 4 nm) WSe_2, Sb_2Se_3, Bi_2Te_3 nanosheets can also been obtained (**Supplementary Fig. 2**). The elemental composition and valence (**Fig. 8**), electronic structure (**Fig. 9a-d**), and photon absorption property (**Fig. 9e-h**) of the exfoliated nanosheets are also provided.
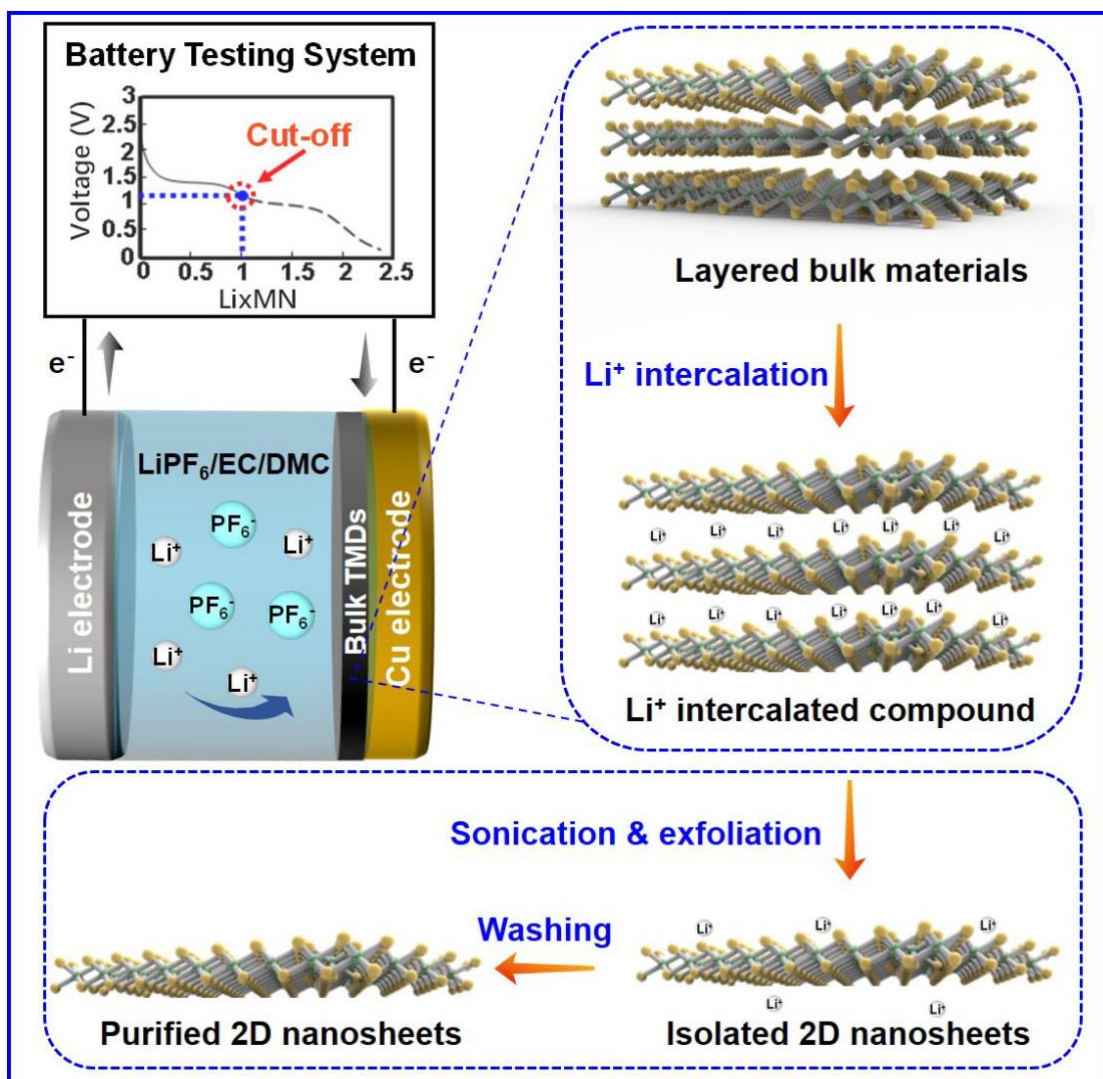
Figure 1 Schematic illustrations of the electrochemical lithium ion-intercalation and exfoliation process.

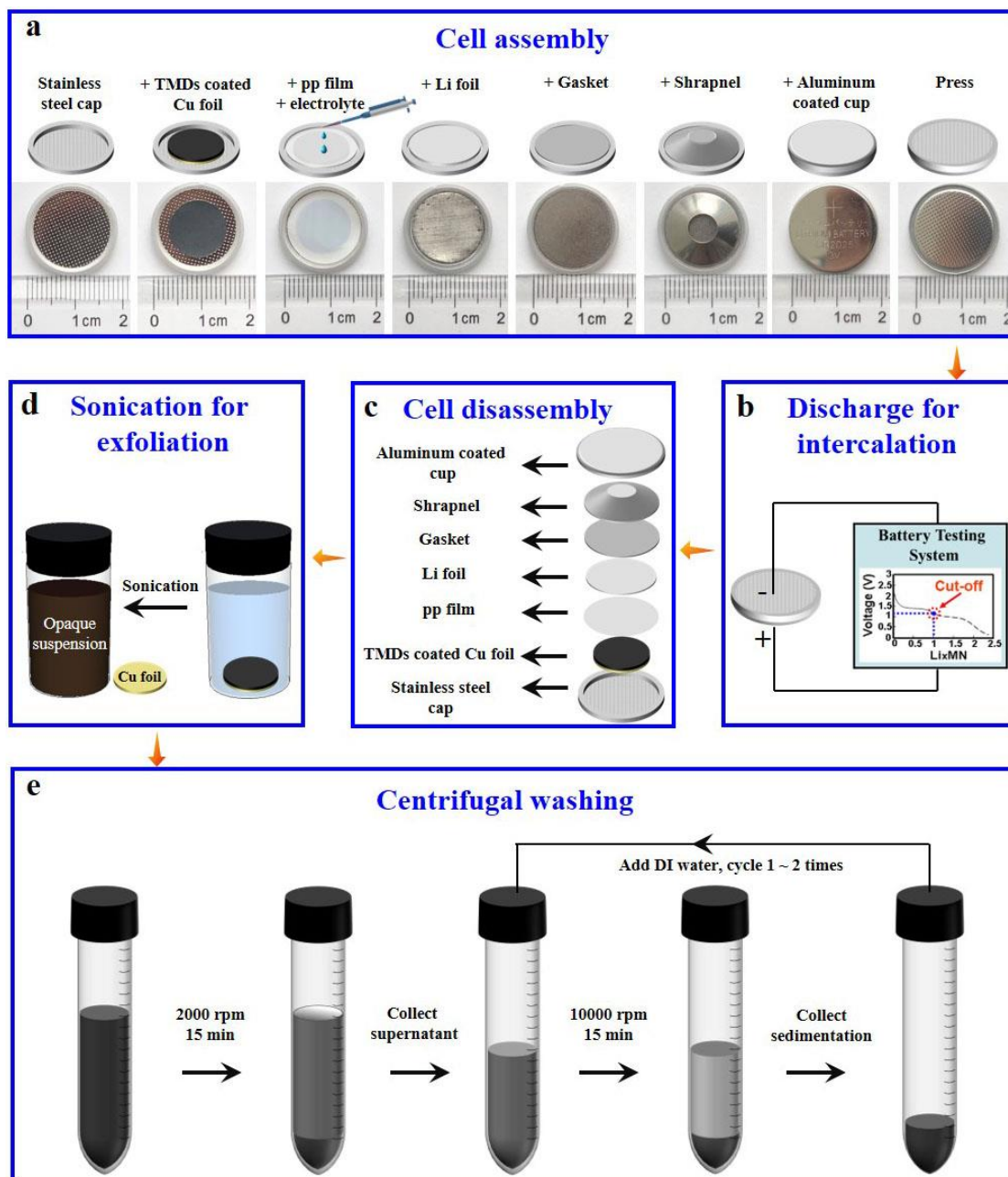**Figure 2** A photograph of the electrochemical lithium ion-intercalation experimental setup (battery test system).

Figure 3 Schematic illustrations of the whole procedures for the preparation of mono- or few- layer TMDs nanosheets.
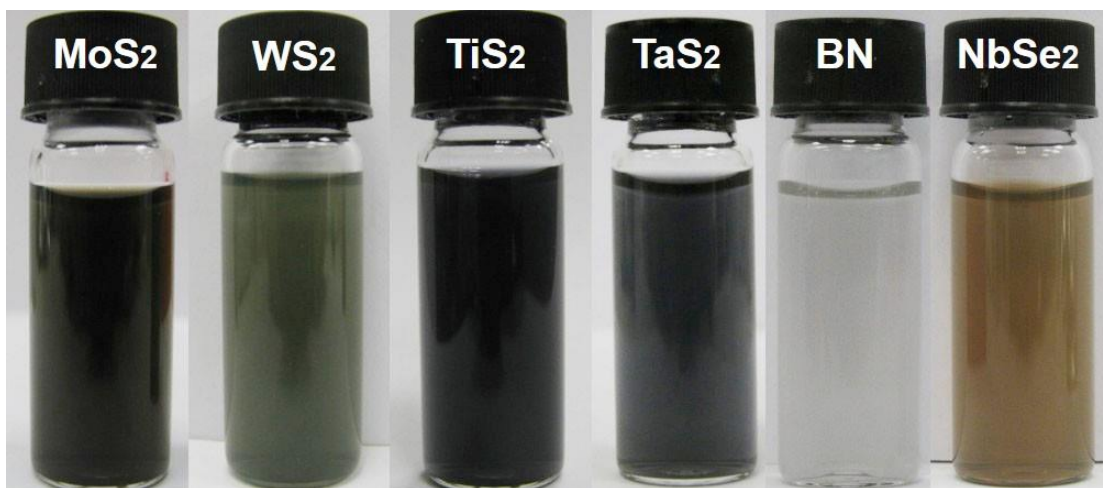
Figure 4 Photographs of the opaque suspension of the exfoliated MoS_2, WS_2, TiS_2, TaS_2, BN, and $NbSe_2$ nanosheets. Adapted with permission from ref. [53,54].
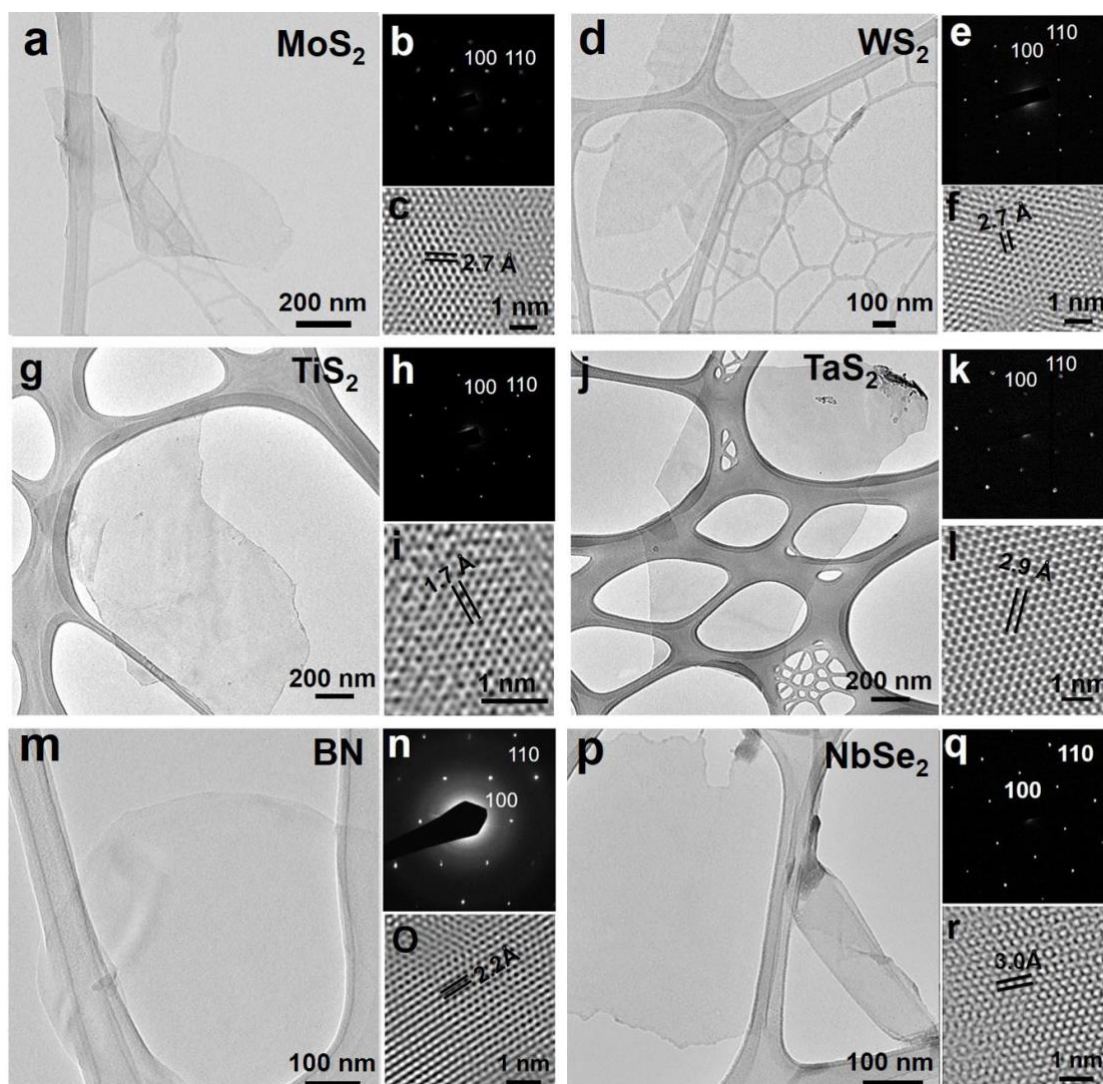

Figure 5 TEM images, selected area electron diffraction (SAED) patterns, and high-resolution transmission electron microscopy (HRTEM) images of the exfoliated MoS_2

(a-c), WS$_2$ (d-f), TiS$_2$ (g-i), TaS$_2$ (j-l), BN (m-o) and NbSe$_2$ (p-r) nanosheets. Adapted with permission from ref. [53,54].
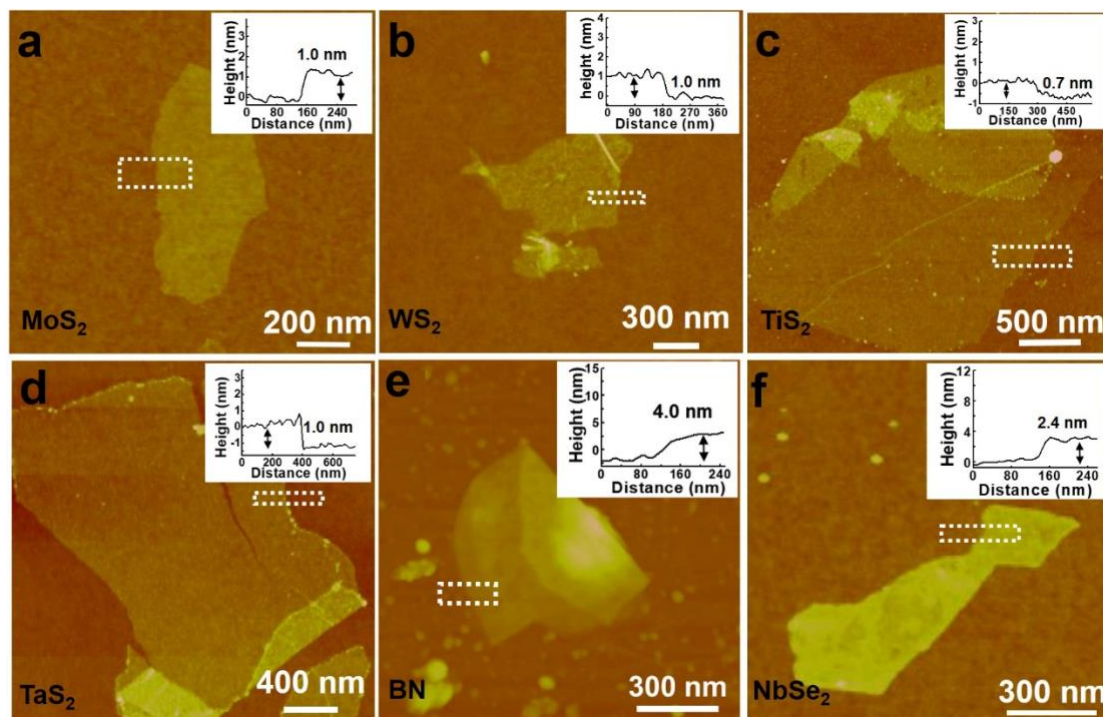

Figure 6 AFM images of the exfoliated MoS$_2$ (a), WS$_2$ (b), TiS$_2$ (c), TaS$_2$ (d), BN (e), NbSe$_2$ (f) nanosheets, giving an average thickness for MoS$_2$, WS$_2$, TiS$_2$, TaS$_2$, BN, NbSe$_2$ nanosheets of ~1.0, 1.0, 0.7, 1.0, 4.0, 2.4 nm, respectively, confirming that mono or few layer inorganic nanosheets were successfully produced by our method. Adapted with permission from ref. [53,54].
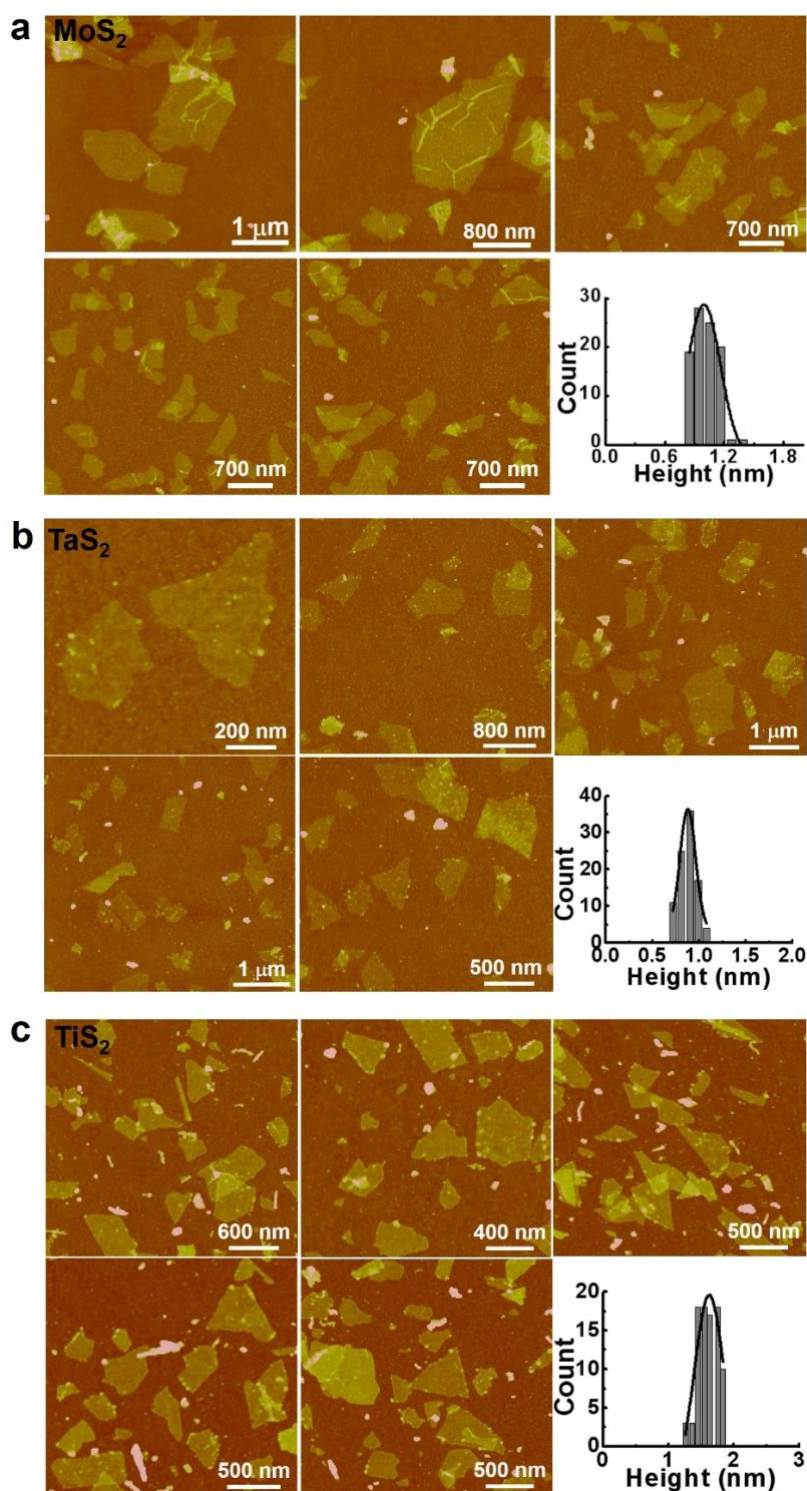
Figure 7 AFM images of large-area MoS_2 (a), TaS_2 (b), TiS_2 (c) nanosheets. By measuring 100 pieces of MoS_2, TaS_2, and TiS_2 nanosheets, respectively. It is found that 92% of MoS_2 are mono layer with the average thickness of 0.99 ± 0.17 nm; 93% of TaS_2 are mono layer with the average thickness of 0.88 ± 0.08 nm; 93% of TiS_2 are double layers with the average thickness of 1.63 ± 0.23 nm. Adapted with permission from ref. [53,55].
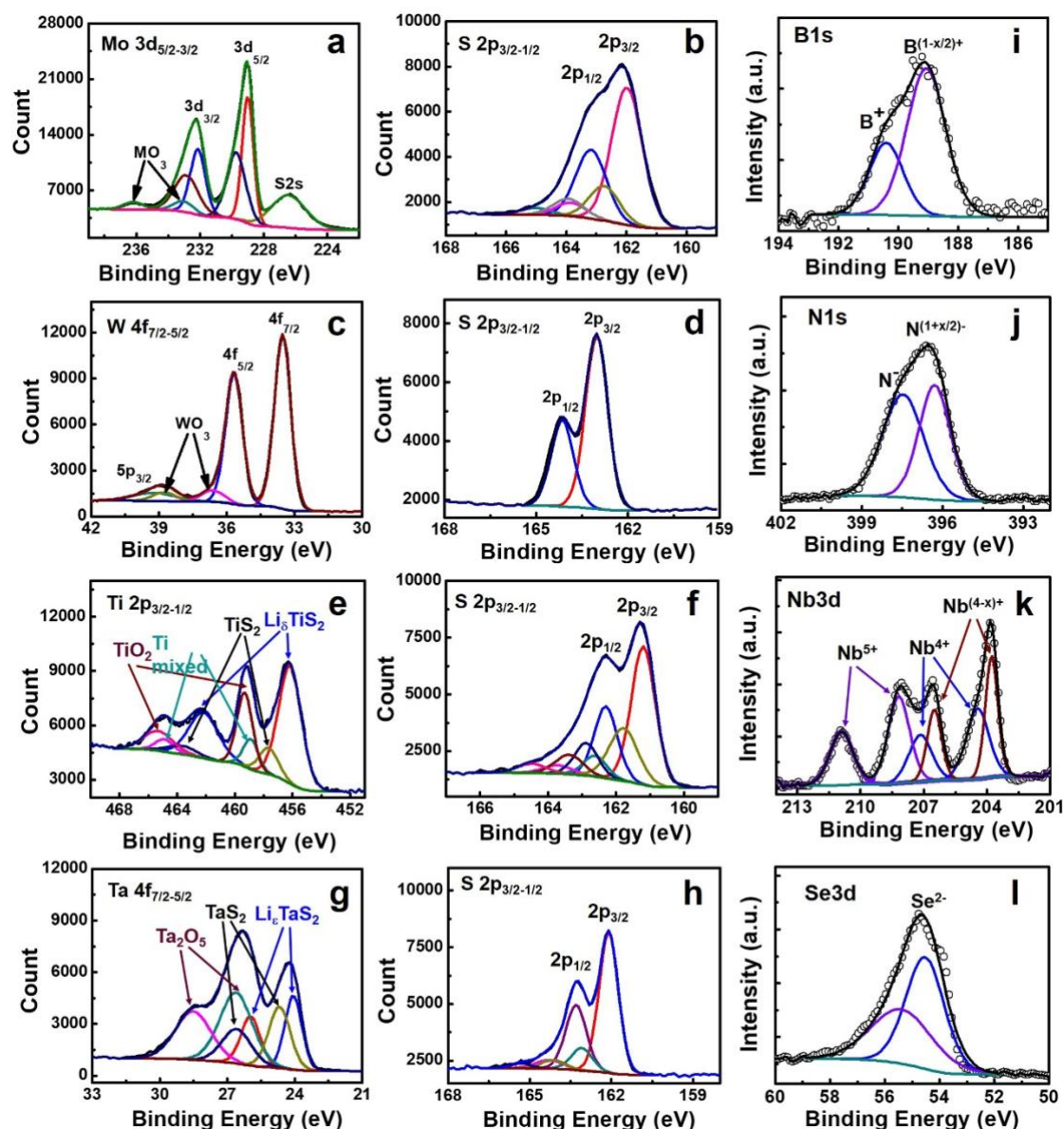
Figure 8 XPS spectra of the exfoliated (a, b) MoS$_2$. 229.0-232.1 eV: Mo3d oxidation state of Li$_x$MoS$_2$. 229.7-232.9 eV: Mo^{4+} of MoS$_2$. 233.0-236.2 eV: Mo^{6+} of MoO$_3$. 162.7-163.9 eV: S^{2-} of MoS$_2$. 163.8-165.0 eV: S$_2^{2-}$ of MoS$_3$. 162.0- 163.2 eV: S2p oxidation state as in Li$_x$MoS$_2$. (c, d) WS$_2$. 33.5 - 35.7 eV: W^{4+} of WS$_2$. 36.6-38.7 eV: W^{6+} of WO$_3$. 163.0-164.2 eV: S^{2-} of WS$_2$. (e, f) TiS$_2$. 456.2-462.2 eV: Ti2p oxidation state as in Li$_x$TiS$_2$. 457.7-463.7 eV: Ti^{4+} of TiS$_2$. 458.9-464.9 eV: Ti2p oxidation state as in mixed environment; 459.3-465.3 eV: Ti^{4+} of TiO$_2$. 161.2-162.3 eV: S2p oxidation state as in Li$_x$TiS$_2$. 161.8-162.9 eV: S^{2-} of TiS$_2$. 162.6-163.7 eV: S$^{4/y}$ of TiS$_y$ (1 < y < 2). 163.4-164.5 eV: S$_2^{2-}$ of TiS$_3$. (g, h) TaS$_2$, 24.1-26.0 eV: Ta4f oxidation state as in Li$_x$TaS$_2$. 24.7-26.6 eV: Ta^{4+} of TaS$_2$. 26.6-28.5 eV: Ta^{5+} of Ta$_2$O$_5$. 162.1-163.3 eV: S2p oxidation

state as in Li_xTiS_2. 163.1-164.3 eV: S^{2-} of TaS_2. 164.1-165.3 eV: S_2^{2-} of TaS_3. (i, j) BN nanosheets. 189.1 and 190.4 eV: B1s oxidation states in Li_xBN, and BN nanosheets, respectively. 396.3 and 397.5 eV: N1s oxidation states in Li_xBN, and BN nanosheets, respectively. (k, l) $NbSe_2$ nanosheets. 203.8 and 206.5 eV: $Nb^{(4-x)+}$ in Li_xNbSe_2. 204.4 and 207.2 eV: Nb^{4+} in $NbSe_2$. 208.1 and 210.9 eV: Nb^{5+} in oxidized species of Nb_2O_5 (37 atomic %). 54.6 and 55.5 eV: Se^{2-} in $NbSe_2$, indicating that selenium is not oxidized. Adapted with permission from ref. [53-55].
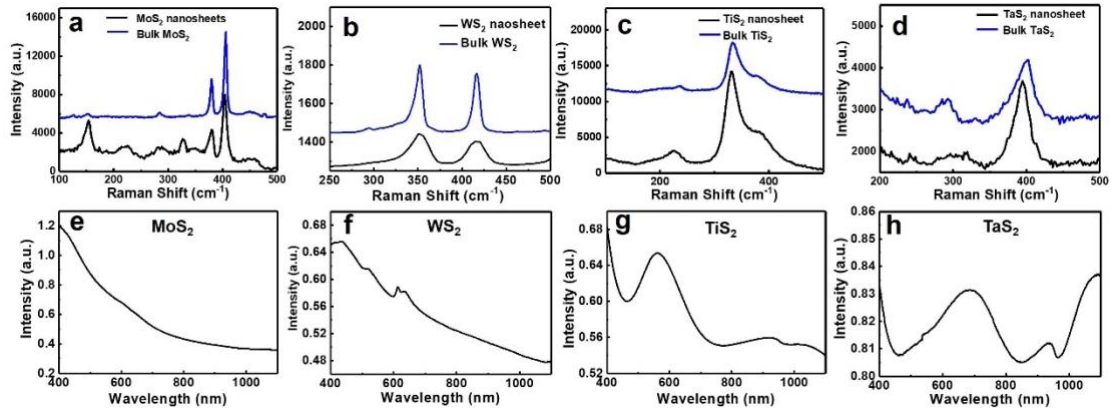

Figure 9 (a) Raman spectra of MoS_2. 379.8 and 406.5 cm^{-1}: E_{2g} and A_{1g} modes of MoS_2 nanosheets with full width at half maximum (FWHM) of 10.4 and 16.0 cm^{-1}, respectively. 379.8 and 406.5 cm^{-1}: E_{2g} and A_{1g} modes of bulk MoS_2 with FWHM of 8.6 and 14.3 cm^{-1}, respectively. MoS_2 nanosheet shows much broader bands compared to the bulk MoS_2, which is owing to the phonon confinement in the ultra-thin structure. Importantly, in the Raman spectra of MoS_2 nanosheets, three weak but distinct new peaks J_1 (153 cm^{-1}), J_2 (225 cm^{-1}) and J_3 (327 cm^{-1}) appeared, illustrating that in addition to pristine 2H phase, the 1T phase also existed in the exfoliated MoS_2 nanosheets. (b) Raman spectra of WS_2. 351 and 415 cm^{-1}: E_{2g} and A_{1g} modes of WS_2 nanosheets with FWHM of 24.6 and 22.3 cm^{-1}, respectively. 352 and 417 cm^{-1}: E_{2g} and A_{1g} modes of bulk WS_2 with FWHM of 10 and 9.2 cm^{-1}, respectively. (c) Raman spectra of TiS_2. 225.2 and 331.3 cm^{-1}: E_g and A_{1g} modes of TiS_2 nanosheets with FWHM of 36.3 and 34.6 cm^{-1}, respectively. 235.3 and 334.4 cm^{-1}: E_g and A_{1g} modes of bulk TiS_2 with FWHM of 16.2 and 31.3 cm^{-1}, respectively. (d) Raman spectra of TaS_2. 300.1 and 395.2 cm^{-1}: E_{2g} and A_{1g} modes of TaS_2 nanosheets with FWHM of 33.2 and 35.0 cm^{-1},

respectively. 289.3 and 401.2 cm^{-1}: E_{2g} and A_{1g} modes of bulk TaS_2 with FWHM of 17.2 and 37.2 cm^{-1}, respectively. Absorbance spectrum for exfoliated dispersions of (e) MoS_2, (f) WS_2, (g) TiS_2, (h) TaS_2 nanosheets. No obvious absorption peak is observed for mono-layer MoS_2 dispersion, but the absorption increases gradually as the wavelength decreases down to 400 nm. Four peaks are observed for mono-layer WS_2 dispersion, which are located at 437, 518, 614, 634 nm, respectively. For TiS_2, three peaks: 561, 930, 1043 nm are presented. The same, there are three peaks located at 689, 936, 1095 nm, which are attributed to exfoliated TaS_2 nanosheets. Adapted with permission from ref. [53].

Acknowledgements

Author contributions

Z.Y. Zeng designed and performed the research; and all authors contributed to writing the manuscript.

Competing interests

The authors declare no competing interests.

Key references using this protocol

Huang, X. et al. *Nat. Commun*. **4**, 1444 (2013), https://www.nature.com/articles/ncomms2472#citeas.

Zhu, C. et al. *J. Am. Chem. Soc*. **135**, 5998-6001 (2013), https://pubs.acs.org/doi/10.1021/ja4019572.

Mei, L. et al. *Chem. Commun.* **57**, 2879 (2021), https://doi.org/10.1039/D0CC08091H.

Key data used in this protocol

Zeng, Z. et al. *Angew. Chem. Int. Ed*. **50**, 11093-11097 (2011),

https://onlinelibrary.wiley.com/doi/10.1002/anie.201106004.

Zeng, Z. et al. *Angew. Chem. Int. Ed*. **51**, 9052-9056 (2012), https://onlinelibrary.wiley.com/doi/full/10.1002/anie.201204208.

Zeng, Z. et al. *Energy Environ. Sci.* **7**, 797-803 (2014), https://doi.org/10.1039/C3EE42620C.

Supplementary information

Supplementary Information: Supplementary Figures 1-8 and Supplementary Tables 1-2.

References

1   Wang, Q. H., Kalantar-Zadeh, K., Kis, A., Coleman, J. N. & Strano, M. S. Electronics and optoelectronics of two-dimensional transition metal dichalcogenides. *Nature Nanotechnology* **7**, 699-712, doi:10.1038/nnano.2012.193 (2012).

2   Xu, X., Yao, W., Xiao, D. & Heinz, T. F. Spin and pseudospins in layered transition metal dichalcogenides. *Nature Physics* **10**, 343-350, doi:10.1038/nphys2942 (2014).

3   Deng, Z. *et al.* 3D Ordered Macroporous MoS2@C Nanostructure for Flexible Li-Ion Batteries. *Advanced Materials* **29**, 1603020, doi:https://doi.org/10.1002/adma.201603020 (2017).

4   Desai, S. B. *et al.* MoS$_2$ transistors with 1-nanometer gate lengths. **354**, 99-102, doi:10.1126/science.aah4698 %J Science (2016).

5   Mak, K. F. & Shan, J. Photonics and optoelectronics of 2D semiconductor transition metal dichalcogenides. *Nature Photonics* **10**, 216-226, doi:10.1038/nphoton.2015.282 (2016).

6   Joensen, P., Frindt, R. F. & Morrison, S. R. Single-layer MoS2. *Materials Research Bulletin* **21**, 457-461, doi:https://doi.org/10.1016/0025-5408(86)90011-5 (1986).

7   Tenne, R., Margulis, L., Genut, M. & Hodes, G. Polyhedral and cylindrical

structures of tungsten disulphide. *Nature* **360**, 444-446, doi:10.1038/360444a0 (1992).

8   Wilson, J. A. & Yoffe, A. D. The transition metal dichalcogenides discussion and interpretation of the observed optical, electrical and structural properties. *Adv Phys* **18**, 193-335, doi:10.1080/00018736900101307 (1969).

9   Koppens, F. H. L. *et al.* Photodetectors based on graphene, other two-dimensional materials and hybrid systems. *Nature Nanotechnology* **9**, 780-793, doi:10.1038/nnano.2014.215 (2014).

10   Manzeli, S., Ovchinnikov, D., Pasquier, D., Yazyev, O. V. & Kis, A. 2D transition metal dichalcogenides. *Nature Reviews Materials* **2**, 17033, doi:10.1038/natrevmats.2017.33 (2017).

11   Zhao, X. *et al.* Engineering covalently bonded 2D layered materials by self-intercalation. *Nature* **581**, 171-177, doi:10.1038/s41586-020-2241-9 (2020).

12   Liu, Y. *et al.* Self-optimizing, highly surface-active layered metal dichalcogenide catalysts for hydrogen evolution. *Nature Energy* **2**, 17127, doi:10.1038/nenergy.2017.127 (2017).

13   Voiry, D. *et al.* Enhanced catalytic activity in strained chemically exfoliated WS2 nanosheets for hydrogen evolution. *Nature Materials* **12**, 850-855, doi:10.1038/nmat3700 (2013).

14   Liu, X.-C. *et al.* Spontaneous self-intercalation of copper atoms into transition metal dichalcogenides. *Science Advances* **6**, eaay4092, doi:10.1126/sciadv.aay4092 %J (2020).

15   Yu, Y. *et al.* Gate-tunable phase transitions in thin flakes of 1T-TaS2. *Nature Nanotechnology* **10**, 270-276, doi:10.1038/nnano.2014.323 (2015).

16   Ye, J. T. *et al.* Superconducting Dome in a Gate-Tuned Band Insulator. *Science* **338**, 1193-1196, doi:10.1126/science.1228006 %J (2012).

17   Zhao, B. *et al.* High-order superlattices by rolling up van der Waals heterostructures. *Nature* **591**, 385-390, doi:10.1038/s41586-021-03338-0 (2021).

18   Li, B. *et al.* Van der Waals epitaxial growth of air-stable CrSe2 nanosheets with

thickness-tunable magnetic order. *Nature Materials*, doi:10.1038/s41563-021-00927-2 (2021).

19   Li, J. *et al.* General synthesis of two-dimensional van der Waals heterostructure arrays. *Nature* **579**, 368-374, doi:10.1038/s41586-020-2098-y (2020).

20   Kong, L. *et al.* Doping-free complementary WSe2 circuit via van der Waals metal integration. *Nature Communications* **11**, 1866, doi:10.1038/s41467-020-15776-x (2020).

21   Chhowalla, M. *et al.* The chemistry of two-dimensional layered transition metal dichalcogenide nanosheets. *Nature Chemistry* **5**, 263-275, doi:10.1038/nchem.1589 (2013).

22   Xi, X. *et al.* Ising pairing in superconducting NbSe2 atomic layers. *Nature Physics* **12**, 139-143, doi:10.1038/nphys3538 (2016).

23   Radisavljevic, B., Radenovic, A., Brivio, J., Giacometti, V. & Kis, A. Single-layer MoS2 transistors. *Nature Nanotechnology* **6**, 147-150, doi:10.1038/nnano.2010.279 (2011).

24   Mak, K. F., Lee, C., Hone, J., Shan, J. & Heinz, T. F. Atomically Thin ${\mathrm{MoS}}_{2}$: A New Direct-Gap Semiconductor. *Phys. Rev. Lett.* **105**, 136805, doi:10.1103/PhysRevLett.105.136805 (2010).

25   Splendiani, A. *et al.* Emerging Photoluminescence in Monolayer MoS2. *Nano Letters* **10**, 1271-1275, doi:10.1021/nl903868w (2010).

26   Zhou, J. *et al.* A library of atomically thin metal chalcogenides. *Nature* **556**, 355-359, doi:10.1038/s41586-018-0008-3 (2018).

27   Wang, H. *et al.* High-quality monolayer superconductor NbSe2 grown by chemical vapour deposition. *Nature Communications* **8**, 394, doi:10.1038/s41467-017-00427-5 (2017).

28   Lin, H. *et al.* Growth of environmentally stable transition metal selenide films. *Nature Materials* **18**, 602-607, doi:10.1038/s41563-019-0321-8 (2019).

29   Najmaei, S. *et al.* Vapour phase growth and grain boundary structure of molybdenum disulphide atomic layers. *Nature Materials* **12**, 754-759, doi:10.1038/nmat3673 (2013).

30   Lee, Y.-H. *et al.* Synthesis of Large-Area MoS2 Atomic Layers with Chemical Vapor Deposition. *Advanced Materials* **24**, 2320-2325, doi:https://doi.org/10.1002/adma.201104798 (2012).

31   Feldman, Y., Wasserman, E., Srolovitz, D. J. & Tenne, R. High-Rate, Gas-Phase Growth of MoS2 Nested Inorganic Fullerenes and Nanotubes. *Science* **267**, 222-225, doi:10.1126/science.267.5195.222 %J (1995).

32   van der Zande, A. M. *et al.* Grains and grain boundaries in highly crystalline monolayer molybdenum disulphide. *Nature Materials* **12**, 554-561, doi:10.1038/nmat3633 (2013).

33   Shi, J. *et al.* Two-dimensional metallic tantalum disulfide as a hydrogen evolution catalyst. *Nature Communications* **8**, 958, doi:10.1038/s41467-017-01089-z (2017).

34   Gong, Y. *et al.* Spatially controlled doping of two-dimensional SnS2 through intercalation for electronics. *Nature Nanotechnology* **13**, 294-299, doi:10.1038/s41565-018-0069-3 (2018).

35   Ugeda, M. M. *et al.* Characterization of collective ground states in single-layer NbSe2. *Nature Physics* **12**, 92-97, doi:10.1038/nphys3527 (2016).

36   Ge, J.-F. *et al.* Superconductivity above 100 K in single-layer FeSe films on doped SrTiO3. *Nature Materials* **14**, 285-289, doi:10.1038/nmat4153 (2015).

37   Barja, S. *et al.* Charge density wave order in 1D mirror twin boundaries of single-layer MoSe2. *Nature Physics* **12**, 751-756, doi:10.1038/nphys3730 (2016).

38   Ugeda, M. M. *et al.* Giant bandgap renormalization and excitonic effects in a monolayer transition metal dichalcogenide semiconductor. *Nature Materials* **13**, 1091-1095, doi:10.1038/nmat4061 (2014).

39   Mahler, B., Hoepfner, V., Liao, K. & Ozin, G. A. Colloidal Synthesis of 1T-WS2 and 2H-WS2 Nanosheets: Applications for Photocatalytic Hydrogen Evolution. *Journal of the American Chemical Society* **136**, 14121-14127, doi:10.1021/ja506261t (2014).

40   Yoo, D., Kim, M., Jeong, S., Han, J. & Cheon, J. Chemical Synthetic Strategy

for Single-Layer Transition-Metal Chalcogenides. *Journal of the American Chemical Society* **136**, 14670-14673, doi:10.1021/ja5079943 (2014).

41 Lin, Z. *et al.* Solution-processable 2D semiconductors for high-performance large-area electronics. *Nature* **562**, 254-258, doi:10.1038/s41586-018-0574-4 (2018).

42 Cullen, P. L. *et al.* Ionic solutions of two-dimensional materials. *Nature Chemistry* **9**, 244-249, doi:10.1038/nchem.2650 (2017).

43 Eda, G. *et al.* Photoluminescence from Chemically Exfoliated MoS2. *Nano Letters* **11**, 5111-5116, doi:10.1021/nl201874w (2011).

44 Kappera, R. *et al.* Phase-engineered low-resistance contacts for ultrathin MoS2 transistors. *Nature Materials* **13**, 1128-1134, doi:10.1038/nmat4080 (2014).

45 Li, J. *et al.* Printable two-dimensional superconducting monolayers. *Nature Materials* **20**, 181-187, doi:10.1038/s41563-020-00831-1 (2021).

46 Zheng, J. *et al.* High yield exfoliation of two-dimensional chalcogenides using sodium naphthalenide. *Nature Communications* **5**, 2995, doi:10.1038/ncomms3995 (2014).

47 Chou, S. S. *et al.* Controlling the Metal to Semiconductor Transition of MoS2 and WS2 in Solution. *Journal of the American Chemical Society* **137**, 1742-1745, doi:10.1021/ja5107145 (2015).

48 Chou, S. S. *et al.* Chemically Exfoliated MoS2 as Near-Infrared Photothermal Agents. *Angewandte Chemie International Edition* **52**, 4160-4164, doi:https://doi.org/10.1002/anie.201209229 (2013).

49 Chou, S. S. *et al.* Ligand Conjugation of Chemically Exfoliated MoS2. *Journal of the American Chemical Society* **135**, 4584-4587, doi:10.1021/ja310929s (2013).

50 Coleman, J. N. *et al.* Two-Dimensional Nanosheets Produced by Liquid Exfoliation of Layered Materials. *Science* **331**, 568-571, doi:10.1126/science.1194975 %J (2011).

51 Feng, J. *et al.* Metallic Few-Layered VS2 Ultrathin Nanosheets: High Two-Dimensional Conductivity for In-Plane Supercapacitors. *Journal of the*

American Chemical Society **133**, 17832-17838, doi:10.1021/ja207176c (2011).

52   Wan, C. *et al.* Flexible n-type thermoelectric materials by organic intercalation of layered transition metal dichalcogenide TiS2. *Nature Materials* **14**, 622-627, doi:10.1038/nmat4251 (2015).

53   Zeng, Z. *et al.* Single-Layer Semiconducting Nanosheets: High-Yield Preparation and Device Fabrication. *Angewandte Chemie International Edition* **50**, 11093-11097, doi:10.1002/anie.201106004 (2011).

54   Zeng, Z. *et al.* An Effective Method for the Fabrication of Few-Layer-Thick Inorganic Nanosheets. *Angewandte Chemie International Edition* **51**, 9052-9056, doi:https://doi.org/10.1002/anie.201204208 (2012).

55   Zeng, Z., Tan, C., Huang, X., Bao, S. & Zhang, H. Growth of noble metal nanoparticles on single-layer TiS2 and TaS2 nanosheets for hydrogen evolution reaction. *Energy & Environmental Science* **7**, 797-803, doi:10.1039/C3EE42620C (2014).

56   Tan, C. *et al.* Liquid-Phase Epitaxial Growth of Two-Dimensional Semiconductor Hetero-nanostructures. *Angewandte Chemie International Edition* **54**, 1841-1845, doi:10.1002/anie.201410890 (2015).

57   Kumbhakar, P. *et al.* Emerging 2D metal oxides and their applications. *Mater. Today* **45**, 142-168, doi:https://doi.org/10.1016/j.mattod.2020.11.023 (2021).

58   Zhu, J. *et al.* Layer-by-Layer Assembled 2D Montmorillonite Dielectrics for Solution-Processed Electronics. *Advanced Materials* **28**, 63-68, doi:https://doi.org/10.1002/adma.201504501 (2016).

59   Yang, R. *et al.* MnO2-Based Materials for Environmental Applications. *Advanced Materials* **33**, 2004862, doi:https://doi.org/10.1002/adma.202004862 (2021).

60   Zhang, Q., Mei, L., Cao, X., Tang, Y. & Zeng, Z. Intercalation and exfoliation chemistries of transition metal dichalcogenides. *Journal of Materials Chemistry A* **8**, 15417-15444, doi:10.1039/D0TA03727C (2020).

61   He, Q. *et al.* Fabrication of Flexible MoS2 Thin-Film Transistor Arrays for Practical Gas-Sensing Applications. *Small* **8**, 2994-2999,

doi:https://doi.org/10.1002/smll.201201224 (2012).

62   Yin, Z. *et al.* Memory Devices Using a Mixture of MoS2 and Graphene Oxide as the Active Layer. *Small* **9**, 727-731, doi:https://doi.org/10.1002/smll.201201940 (2013).

63   Zhu, C. *et al.* Single-Layer MoS2-Based Nanoprobes for Homogeneous Detection of Biomolecules. *Journal of the American Chemical Society* **135**, 5998-6001, doi:10.1021/ja4019572 (2013).

64   Huang, X. *et al.* Solution-phase epitaxial growth of noble metal nanostructures on dispersible single-layer molybdenum disulfide nanosheets. *Nature Communications* **4**, 1444, doi:10.1038/ncomms2472 (2013).

65   Mei, L. *et al.* Size-selective synthesis of platinum nanoparticles on transition-metal dichalcogenides for the hydrogen evolution reaction. *Chemical Communications*, doi:10.1039/D0CC08091H (2021).

66   Yin, Z. *et al.* Preparation of MoS2–MoO3 Hybrid Nanomaterials for Light-Emitting Diodes. *Angewandte Chemie International Edition* **53**, 12560-12565, doi:https://doi.org/10.1002/anie.201402935 (2014).

67   Zeng, Z. *et al.* In Situ Study of Lithiation and Delithiation of MoS2 Nanosheets Using Electrochemical Liquid Cell Transmission Electron Microscopy. *Nano Letters* **15**, 5214-5220, doi:10.1021/acs.nanolett.5b02483 (2015).

68   Yang, H., Kim, S. W., Chhowalla, M. & Lee, Y. H. Structural and quantum-state phase transitions in van der Waals layered materials. *Nature Physics* **13**, 931-937, doi:10.1038/nphys4188 (2017).

69   Voiry, D., Mohite, A. & Chhowalla, M. Phase engineering of transition metal dichalcogenides. *Chemical Society Reviews* **44**, 2702-2712, doi:10.1039/C5CS00151J (2015).

70   Li, W., Qian, X. & Li, J. Phase transitions in 2D materials. *Nature Reviews Materials*, doi:10.1038/s41578-021-00304-0 (2021).

71   Heising, J. & Kanatzidis, M. G. Structure of Restacked MoS2 and WS2 Elucidated by Electron Crystallography. *Journal of the American Chemical Society* **121**, 638-643, doi:10.1021/ja983043c (1999).

72   Voiry, D., Drummond, C. & Pénicaud, A. Portrait of carbon nanotube salts as soluble polyelectrolytes. *Soft Matter* **7**, 7998-8001, doi:10.1039/C1SM05959A (2011).